High Performance and Stability in COMPASS-D

B. Lloyd, L. Appel, K.B. Axon, C.A. Bunting, R.J. Buttery, P.G. Carolan, N.J. Conway, G. Cunningham, J. Dowling, M.R. Dunstan, T. Edlington, A.R. Field, S.J. Fielding, S.J. Manhood, K.G. McClements, H.F. Meyer, A.W. Morris, M.R. O'Brien, T. Pinfold, V. Shevchenko, K. Stammers, M.R. Tournianski, M. Valovic, M.J. Walsh 1), C.D. Warrick, H.R. Wilson and the COMPASS-D and ECRH Teams.

EURATOM/UKAEA Fusion Association, Culham Science Centre,
Abingdon, Oxon, OX14 3DB, UK

1) Walsh Scientific Ltd, Culham Science Centre, Abingdon, Oxon, OX14 3EB, UK

e-mail contact of main author: brian.lloyd@ukaea.org.uk

Abstract. COMPASS-D is a compact, adaptable, D-shaped tokamak equipped with powerful heating (ECRH) and current drive (LHCD/ECCD) systems allowing access to both H-mode (ELMy and ELM-free) and quasi-stationary high beta regimes under conditions of dominant electron heating ($T_e > T_i$), negligible external momentum input and no central fuelling. Control and avoidance of neo-classical tearing modes (NTMs) has enabled quasi-stationary high beta ($\beta_N \sim 2$, $\beta_p > 1$) discharges to be sustained for ~ 20 energy confinement times and a duration corresponding to 20% of that of a nominal ITER discharge, when normalised to the current diffusion time. Controlled seeding of NTMs by external application of resonant magnetic perturbations has enabled NTM onset criteria to be carefully explored and compared with theory; observed island evolutions follow theoretical expectations. Off-axis lower hybrid current drive (LHCD) has been reliably used to completely stabilise NTMs in high beta discharges. Detailed modelling has shown that the stabilising effect is consistent with a reduction in the stability index Δ', although other stabilisation mechanisms may also contribute. High frequency energetic particle driven instabilities (~400kHz), which exhibit frequency-sweeping ('chirping'), have, for the first time, been observed with high power ECRH as the sole source of auxiliary heating.

1. Introduction

Two of the main operating regimes presently foreseen for burning plasma devices such as ITER-FEAT are the ELMy H-mode and the high beta advanced tokamak regime with enhanced confinement and high bootstrap current fraction (f_{BS}). The latter regime offers the potential of steady-state operation. However, the non-linear coupling between pressure and current density profiles is problematic for the steady-state control of such high f_{BS} regimes. Furthermore, neo-classical tearing modes (NTMs) may restrict the achievable plasma beta to values well below the ideal MHD (Troyon) limit, particularly at low collisionality. The understanding of NTM onset criteria and the development of robust methods of NTM control/avoidance are key to achieving reliable access to stationary high beta regimes.

COMPASS-D is a compact, adaptable, D-shaped tokamak (R = 0.56m, a = 0.17m) equipped with powerful heating (ECRH) and current drive (LHCD/ECCD) systems, allowing access to both H-mode (ELMy and ELM-free) and quasi-stationary high beta regimes under conditions of dominant electron heating ($T_e > T_i$), negligible external momentum input and no central fuelling. These conditions are similar to those that will prevail in fusion devices where alpha particle heating is dominant. Extensive H-mode studies have been carried out on COMPASS-D and the latest results are described in a companion paper [1]. High beta regimes, including the study of NTM onset criteria and control schemes, are described in the present paper.

The COMPASS-D 60GHz ECRH system has been used to deliver up to ~ 1.5MW to the tokamak. COMPASS-D is equipped with eleven antennas, five on the high-field-side (HFS) and six on the low-field-side (LFS) of the tokamak. The HFS antennas incorporate rotatable mirrors to allow variation of the toroidal launch angle whereas the LFS antennas are fixed (four orientated to launch waves clockwise and two orientated to launch waves anti-clockwise from above). The polarisation (linear) of the launched waves can be selected by rotation of mode converters in the transmission lines. The gyrotrons can be flexibly configured to a mixture of HFS and LFS antennas depending on the particular experimental requirement and the direction/magnitude of electron cyclotron driven current can be adjusted at fixed heating power. COMPASS-D is also equipped with a 1.3GHz LHCD system. The power is launched via a conventional eight-waveguide grill fed by one or two 300kW, 1.5s klystrons. For a nominal phase difference of 60° between adjacent waveguides, as employed in the experiments described here, the launched spectrum peaks at $N_{\|} \sim 2.1$.

With the available heating power, high beta regimes are only accessible at low toroidal field requiring the use of second harmonic extra-ordinary mode ECRH ($B_{res} = 1.07T$) and hence restricting operation to relatively low density ($n_e < 2.2 \times 10^{19}\ m^{-3}$) to allow wave accessibility. Typical single null divertor (SND) discharge parameters in the experiments described here were thus $B_\phi \sim 1.1 - 1.2T$, $I_p = 120 - 180kA$, $q_{95} \sim 3.2 - 4.1$, $\kappa \sim 1.6$, $\bar{n}_e \sim 1 \times 10^{19}\ m^{-3}$.

2. Background

Profile control is essential for achievement of stationary high beta regimes. Several current profile control techniques have been employed in COMPASS-D for discharge optimisation, viz.,

- ECRH timing/power waveform programming,
- counter-ECCD in the plasma core,
- off-axis LHCD.

The effect on the beta limit of current profile control by ECCD was demonstrated in [2]. The driven current in the plasma core was systematically varied by adjustment of the steerable HFS antennas, whilst keeping the power deposition profile reasonably fixed. Counter-current drive ($j_{ECCD} \sim 0.5MA/m^2$) in the core, which is expected to increase q(0), resulted in a ~ 10% increase in the beta limit ($\beta_N \leq 2.1$, $\beta_p \leq 1.3$) compared with balanced injection, whereas co-current drive led to a ~10% decrease. These high beta discharges were essentially transient, generally ending in disruption preceded by a large predominantly m = 2, n = 1 mode. Calculations with the SCENE code [3] indicated bootstrap current fractions up to f_{BS} ~70% in these discharges and further extensive studies [4] confirmed that neo-classical tearing modes were generally responsible for the observed beta limit. In particular, the observed MHD activity exhibited a number of expected characteristics based on the theory of neo-classical tearing modes, viz.,

- the scaling of the threshold poloidal beta (β_p) for mode onset with density (collisionality),
- the scaling of the saturated island width with β_p during ECRH power (and hence β_p) ramp-down,
- observation of a critical island size below which the modes do not grow.

Techniques developed to avoid or stabilise NTMs in COMPASS-D are described in sections 4 and 5. First we describe recent further detailed studies of the onset criteria.

3. Controlled Seeding of Neo-classical Tearing Modes

Since NTMs present a serious concern for Next Step devices it is important to be able to estimate thresholds for mode onset and to identify likely requirements for stabilisation systems. This in turn requires a thorough understanding of the underlying physics governing mode onset and driving/stabilising mechanisms. A key aspect of the onset criteria for NTMs is the triggering mechanism which requires a finite seed island (generated by sawteeth for example). In the case of “natural” NTMs, it is hard to decouple measurements of the MHD activity involved in mode onset from the seed perturbation itself, making direct verification of the onset criteria difficult. Furthermore, the parameter space which can be explored is limited by the space in which natural seed perturbations occur, preventing a full examination of the onset criteria and their parametric dependencies.

The growth of neoclassical tearing modes can be described by the modified Rutherford equation [5] for an island of size ‘w’:

$$\frac{\tau_r}{r^2}\frac{dw}{dt} = \Delta' + a_{bs}\varepsilon^{1/2}\left(L_q / L_p\right)\frac{\beta_P}{w}\left(\frac{1}{1+w_d^2/w^2} - \frac{w_{pol}^2}{w^2}\right) \tag{1}$$

This is expressed in terms of the stability index Δ', which is negative and therefore stabilising for NTMs, and the bootstrap current ($a_{bs}\beta_p/w$) term [6] which represents the effect of bootstrap current reduction within the island region that drives the NTM growth (a_{bs} is a constant of proportionality). τ_r is proportional to the resistive time scale; ε is the inverse aspect ratio of the resonant surface; L_q and L_p are profile parameters referring to safety factor and pressure gradient scale lengths. Ion polarisation effects [7] (w_{pol} term) and finite island transport effects [8] (w_d term) act to stabilise the mode at small island sizes, giving rise to the requirement for a finite amplitude seed island for NTM growth. Setting dw/dt = 0 in equation (1) gives the minimum β_p for marginal growth as a function of island size (Fig 1a). The exact form of the curve in Fig 1a depends on the relative magnitude and scaling of the ion polarisation and finite island transport terms, regarding which there is still some uncertainty. Nevertheless, it is apparent from Fig 1a that there is a critical seed island size (w_{crit}) below which NTMs are stable at all values of β_p and a critical β_p (β_{crit}) below which NTMs are stable for all seed island sizes.

On COMPASS-D, well-defined measurable seed islands can be created in the plasma using the highly adaptable RMP (resonant magnetic perturbation) external saddle coil set, which can be configured to produce various relatively pure harmonics of magnetic perturbation (in this case m = 2, n = 1) to drive island formation. The RMP coils are used to induce a locked magnetic island in the plasma at low beta. When the currents in the windings are switched off, this island then rapidly “spins-up” to some natural rotation frequency and, at low β_p, starts to decay in amplitude, producing a well-defined rotating mode in the plasma with identifiable structure. Strong heating is then applied, increasing β_p, and observation of the subsequent island evolution allows determination of the criteria (island size and β_p) for which positive neo-classical island growth is obtained (i.e. the “onset” or “threshold” criteria). By varying the timing of the heating ramp during the mode decay an exploration of this parameter space can be made. This allows a controlled study of new areas of parameter space, where the various stabilising terms that are critical in the NTM onset play a crucial role. A set of 28 nominally identical discharges (I_p = 140kA, B_ϕ = 1.1T, κ = 1.6, q_{95} = 3.8) with line-averaged densities in a narrow range ($\bar{n}_e$ ~ 6-7 x 10^{19} m^{-3}) was studied. In excess of 1MW of ECRH power was injected into the plasma using a balanced configuration of launch angles to ensure no net electron cyclotron current drive. The resulting island evolutions are shown in Fig 1b where it is seen that they are in good accord with theoretical expectations as represented in Fig 1a. In particular it may be noted that there is a minimum critical β_p (~ 0.45) for positive growth (marked with a ‘✧’ four point star in Fig 1b). Furthermore it may be seen that discharge trajectories divide neatly into two categories: those that pass to the right of the star

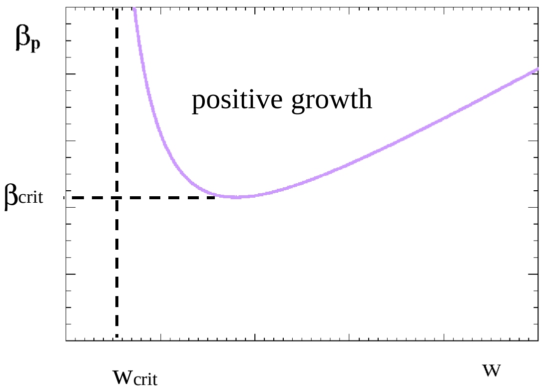

Fig 1a Minimum b_p for marginal NTM growth versus island width w.

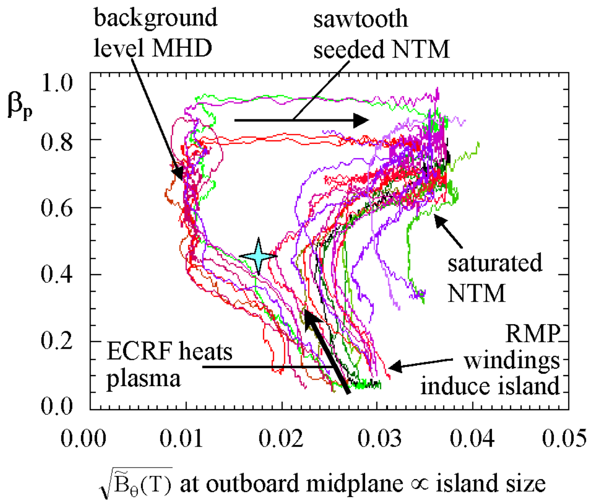

Fig 1b Evolution of rmp induced island with ECRH for 28 nominally identical discharges (varied ECRH timing).

(resulting in an NTM which limits the achievable beta) and others that go to the left (no-NTM) where measured amplitudes decay to some background level and beta increases significantly. In the latter case an NTM may eventually be triggered by some ‘natural’ perturbation (e.g. sawtooth) which produces a seed island in excess of the critical value.

4. Stabilisation of Neo-classical Tearing Modes by Lower Hybrid Current Drive

It has been proposed that NTMs may be stabilised by local current drive within the magnetic island to replace the “missing” bootstrap current [9]. In addition, co-current drive at, or close to, the mode rational surface can steepen (flatten) the equilibrium current gradients outside (inside) the surface, resulting in a reduction in the free energy available in the equilibrium current profile (parameterised by Δ') [10].

NTMs (triggered either naturally or using the RMP coils) have been completely stabilised in ECR-heated discharges (q_{95} ~ 3.8) in COMPASS-D with modest levels (80 – 120kW) of launched LHCD power, corresponding to only ~ 10% of the total input power [11]. Again, a balanced configuration of ECRH launch angles was used to ensure no net electron cyclotron current drive. An example is shown in Figure 2 where a naturally triggered neo-classical mode (observed in the m = even, n = odd component of the perturbed poloidal magnetic field) is completely removed by LHCD with P_{LH} = 90kW. Removal of the mode occurs ~ 10ms after the start of the LHCD pulse, consistent with estimates of the diffusion time for the LH driven current perturbation (~ 7ms). The initial appearance of the mode is characterised by a clear saturation of β_p which persists into the LHCD pulse. The LH flat-top phase is accompanied by a loss of ECRH power (~ 130kW) from one of the gyrotrons (caused by

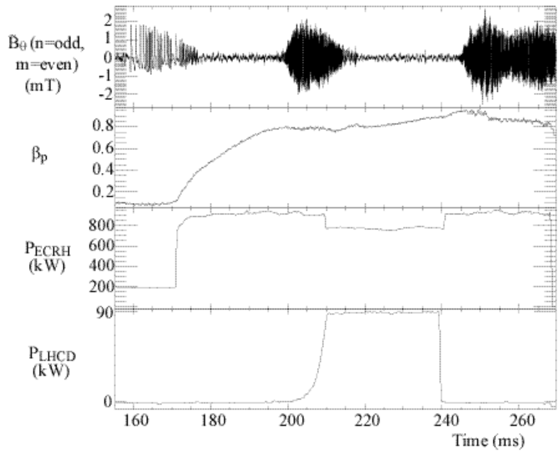

Fig 2 NTM stabilisation by LHCD (#28601)

‘pickup’ from the LH system on its reverse power detector). Although not intentional, this does in fact ensure that the total rf input power is maintained at an approximately constant level. The loss of ECRH power in this way causes a negligible initial drop in β_p, which is rapidly followed by a significant increase in β_p (~ 15% in this shot) as the mode is stabilised by the LHCD. The fact that the mode is decaying despite a rise in β_p is clear evidence for LHCD stabilisation. β_p continues to rise (achieving a peak β_p ~ 0.95 and β_N ~ 1.6) until the mode reappears well after the LHCD is turned off. The delay between the end of the LHCD pulse and the reappearance of the neo-classical mode (~5ms in this case) is again consistent with the calculated LH current diffusion time but could also be attributed to the absence of an immediate trigger for the re-growth of the mode.

The LHCD power required for full stabilisation increases with increasing line-averaged density in the narrow operating range $\bar{n}_e$ = 0.6 – 0.8 x 10^{19} m^{-3} consistent with the fact that the magnitude of the LH driven current is the dominant factor in the stabilisation. Low levels of LH power resulted in only partial stabilisation. The reduction in mode amplitude as a function of LH absorbed power (injected LH power minus reflected power) normalised to the line-averaged density is shown in Figure 3. The discontinuous jump in the reduction in mode amplitude as the LH power is increased may be associated with a reduction of the island width below the threshold level allowing the mode to decay naturally.

The LH driven current profile has been calculated (Fig 4) using the relativistic and self-consistent Fokker-Planck and ray tracing code BANDIT-3D [12], using $T_e(r)$ and $n_e(r)$ profiles fitted to Thomson scattering measurements. As seen in Fig 4, the measured $T_e(r)$ profile is strongly peaked during ECRH (T_{e0} ~ 4keV), reflecting the strong damping in the plasma core, whereas the measured $n_e(r)$ profiles are broad. Neither $n_e(r)$ nor $T_e(r)$ profiles show any significant change during the LHCD phase. The calculated LH driven current profile (I_{LH} ~ 20%I_p) is peaked off-axis (r/a ~ 0.6 – 0.85) consistent with the observed reduction in internal inductance deduced from the EFIT equilibrium reconstruction code.

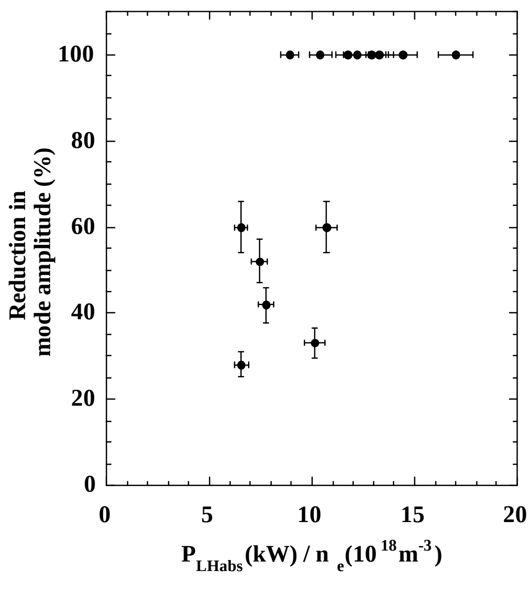

Fig 3 Reduction in mode amplitude as a function of LH power normalised to the line-averaged density.

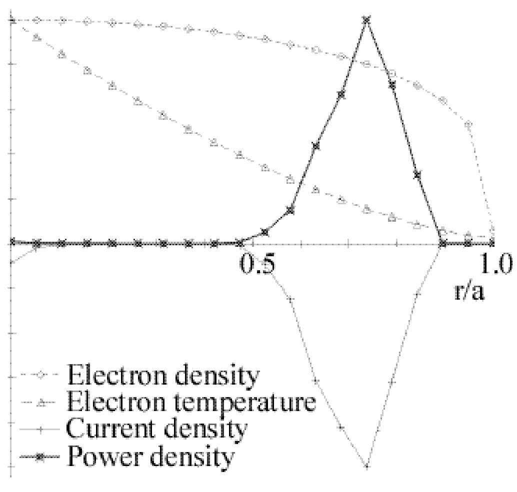

Fig 4 BANDIT-3D calculation of LH absorbed power and current density profiles using experimental density and temperature profiles.

The q = 2 surface is located at r/a ~ 0.7 – 0.8 and calculations show that the NTM stabilisation by LHCD can be explained by a reduction in Δ' arising from LH co-current drive at and around the mode rational surface. A reference equilibrium current profile (no LHCD) was derived using TOPEOL (a free boundary Grad-Shafranov equilibrium solver) carefully matched to an EFIT equilibrium reconstruction (based on experimental data). The LH driven current, determined by BANDIT-3D, was added and the equilibrium re-converged conserving the total plasma current (which is feedback controlled during the experiments). The perturbed current profiles were used to calculate a cylindrical approximation to $r_s\Delta'$ (where r_s is the radius of the q = 2 surface) as a function of the assumed position of the current perturbation peak with respect to the location of the q = 2 surface (Fig 5). As expected, the largest relative reduction in $r_s\Delta'$ (~ - 3) is observed when the centre of the current perturbation is located at, or very close to, the q = 2 surface. Stabilising reductions in $r_s\Delta'$ are obtained when the LH driven current peak is displaced over a range of 3cm around the rational surface. This is equivalent to ~ 17% of the minor radius on COMPASS-D. Indeed, the calculated position of the LH driven current profile from BANDIT-3D (indicated by the diamond in Fig 5) is very close to the evolved position of the q = 2 surface deduced from TOPEOL, resulting in a maximum reduction of $r_s\Delta'$ in these experiments. The effect on the island width evolution of such a relative change in $r_s\Delta'$ was calculated using equation (1) and compared to experimental estimates [11]. Good agreement was found, showing that stabilisation via a modification of Δ' can account for the experimental results, although there are other stabilising mechanisms which could contribute. The removal of the q = 1 surface can have a stabilising influence on the q = 2 surface. Also LHCD contributes to the direct replacement of the missing bootstrap current with driven current within the island. However, the LH driven current profile extends well beyond the island and analytic calculations show that the dominant effect is accounted for in the Δ' calculation with any additional (“non-linear” layer) contribution to equation (1) being small [~ $(w/\delta)^2$ < 15%, where δ is the full width of the LH driven current].

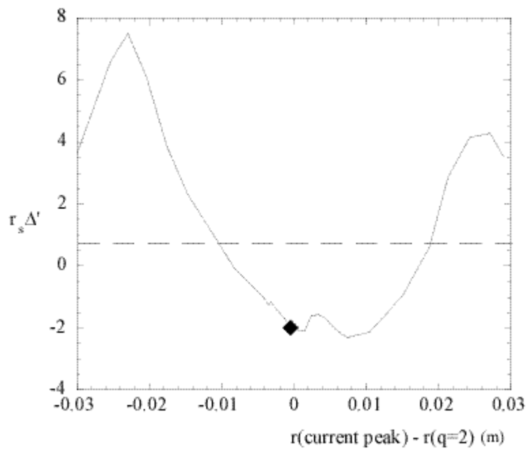

Fig 5 Dependence of r_sD¢ on assumed radial location of LH driven current perturbation. The dotted line indicates the value of r_sD¢ for the unperturbed case and ¨ corresponds to the BANDIT-3D calculation of the driven current location.

5. Development of Quasi-stationary High Beta Discharges

High power ECRH in low q discharges (q_{95} ~ 3), allows access to high beta (β_N > 2) but such discharges always terminate in a disruption, generally caused by an m = 2, n = 1 tearing mode. At higher q (q_{95} ~ 4), the occurrence of an m = 2, n = 1 mode during ECRH may not lead to a disruption but rather to a degradation of energy confinement by 20 – 50% limiting the achievable beta. By discharge optimisation (early x-point formation to reduce MHD activity during the plasma current ramp-up) and optimised programming of the ECRH (maximum power applied near the start of the plasma current flat-top), the m = 2, n = 1 neo-classical tearing mode can be fully avoided and β_N can be raised above 2 and sustained for > 100ms, [13] (Fig 6). Postponing the heating pulse by ~ 10ms resulted in destabilisation of the m = 2, n = 1 tearing mode later in the discharge and hence degraded performance. This strong sensitivity to the timing of the heating pulse is probably related to the target q-profile combined with substantial bootstrap current fraction (f_{BS} ~ 50%). The discharge in Fig 6 is quasi-stationary (~ $18\tau_E$ but shorter than the global current diffusion time) with constant internal inductance and no obvious growth of detrimental MHD instabilities. The plasma is sawtooth-free but the Mirnov signals show regular bursts which have been attributed to energetic particle driven instabilities [13]. These energetic particle driven instabilities are only observed at the highest ECRH powers, although there are indications that LHCD may somewhat reduce the ECRH power required. The repetition time varies from 1 to 5ms. The temporal behaviour of the frequency spectrum of the Mirnov signal during these events is illustrated in Fig 7, where it is seen that each burst consists of multiple "chirps". In this example, triplets are observed but there are also cases with double and single "chirps". There are no signs of reconnection caused by these modes and they cause no observable effects on beta. Analysis of the mode numbers inside the bursts is complicated by the high frequency (up to ~ 450kHz) and incoherence of the Mirnov signals. The observed frequency is close to the toroidal Alfvén eigenmode gap frequency $v_A/(4\pi qR_0)$ ~ 400kHz (for q ~ 1.5); the bursts may be driven by an instability arising from resonance with the precessional drift of energetic trapped electrons ($E_\perp$ ~ 50 – 90keV).

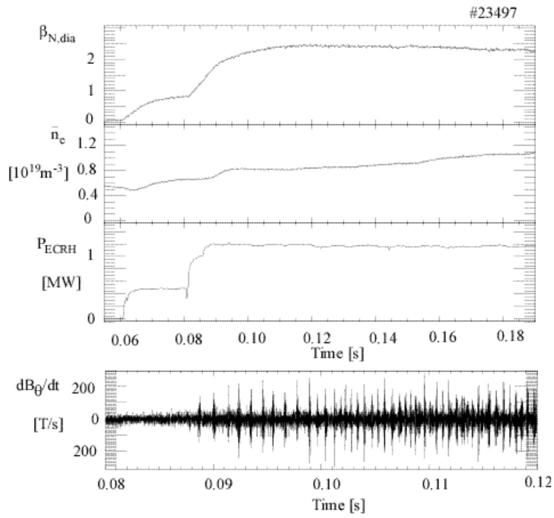

Fig 6 Optimised quasi-stationary high beta ECRH discharge.

At somewhat lower ECRH power (~ 1MW) core relaxations can result in significant modulation (~9%) of the total stored energy [14]. When the heating power is reduced further (~ 0.8MW), the central soft x-ray emission displays a variety of waveforms such as "humpbacks", "inverted sawteeth" and "hills" as observed in the TCV tokamak [15]. At still lower power levels (~ 0.5MW), the usual triangular sawteeth are recovered.

The duration of the high beta phase in ECRH-only plasmas is limited due to a steady decay in beta (see Fig 6) which can be avoided by additional low power LHCD (Fig 8). The high beta phase ($\beta_N \geq 2$) is sustained for ~ $20\tau_E$, until the end of the heating pulse. In low q high beta ECR-heated discharges, which normally disrupt due to m = 2, n = 1 modes, low power LHCD has also been used to delay or avoid disruptions [14, 16]

6. Summary and Conclusions

The control and avoidance of neo-classical tearing modes (NTMs) has enabled quasi-stationary high beta (β_N ~ 2, β_p > 1) discharges to be sustained for ~ 20 energy confinement times and a duration corresponding to 20% of that of a nominal ITER discharge, when normalised to the current diffusion time. Controlled seeding of NTMs by external application of resonant magnetic perturbations has enabled NTM onset criteria to be carefully explored and compared with theory; observed island evolutions follow theoretical expectations. Off-axis lower hybrid current drive (LHCD) has been reliably used to completely stabilise NTMs in high beta discharges. Detailed modelling has shown that the stabilising effect is consistent with a reduction in the stability index Δ', although other stabilisation mechanisms may also contribute. High frequency energetic particle driven instabilities (~400kHz), which exhibit a

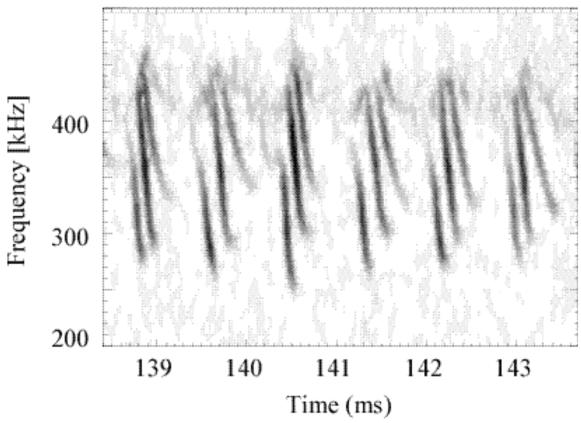

Fig 7 Spectrogram of Mirnov signal showing 'chirping' character of fast particle driven MHD activity.

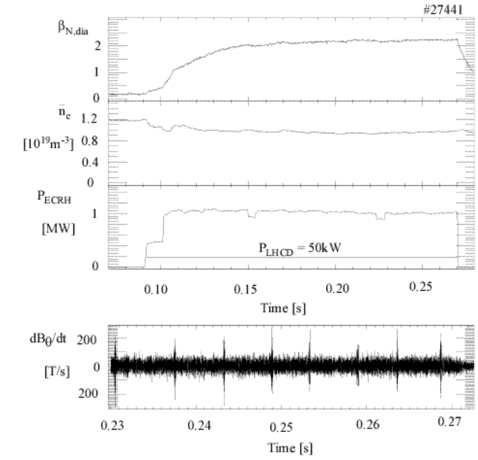

Fig 8 Quasi-stationary high beta discharge with ECRH and LHCD.

'chirping' nature have also been observed, for the first time, with high power ECRH as the sole source of auxiliary heating.

Acknowledgements

This work is funded by the UK Department of Trade and Industry and Euratom. The loan of lower hybrid equipment from IPP Garching and CEA Cadarache is gratefully acknowledged.

References

[1] FIELDING, S.J., et al., "Transition Dynamics and Confinement Scaling in COMPASS-D H-mode Plasmas", Fusion Energy 2000 (Proc. 18th Int. Conf. Sorrento, 2000), IAEA, Vienna (2001) (CD-ROM file EXP 5/29)
[2] GATES, D.A., et al., Proc. 22nd European Conf. on Plasma Phys. and Contr. Fusion, **IV**, (1995) 117.
[3] WILSON, H.R., "SCENE - Simulation of Self-Consistent Equilibria with Neo-classical Effects", UKAEA Fusion Report FUS-271.
[4] GATES, D.A., et al., Nuclear Fusion **37** (1997) 1593.
[5] SAUTER, O., et al., Nuclear Fusion **4** (1997) 1654.
[6] CARRERA, R., et al., Phys. Fluids **29** (1986) 899.
[7] WILSON, H.R., et al., Phys. Plasmas **3** (1996) 248.
[8] FITZPATRICK, R., et al., Phys. Plasmas **2** (1995) 825.
[9] HEGNA, C.C. and CALLEN, J.D., Phys. Plasmas **4** (1997) 2940.
[10] PLETZER, A. and PERKINS, F.W., Phys. Plasmas **6** (1999) 1589.
[11] WARRICK, C.D., et al., Phys. Rev. Lett. **85** (2000) 574.
[12] O'BRIEN, M.R., et al., Proc. of IAEA Tech. Comm. Mtg on Advances in Simulation and Modelling of Thermonuclear Plasmas, Montreal, 1992, IAEA Vienna (1993) 527.
[13] VALOVIC, M., et al., Nuclear Fusion **40** (2000) 1569.
[14] VALOVIC, M., et al., Proc. Eur. Top. Conf. on RF Heating and Current Drive of Fusion Devices, Brussels (1998) 217.
[15] PIETRZYK, Z.A., et al., Nuclear Fusion **39** (1999) 578.
[16] MORRIS, A.W., et al., Fusion Energy 1998 (Proc. 17th IAEA Fusion Energy Conference, Yokohama, 1998) IAEA, Vienna (1999) 773.